quasielastic scattering shown in Fig. 1. The origin of this scattering is not at all understood at present. Moreover, we even failed to characterize this scattering precisely. Its location in energy is well centered at $E = 0$; however, its location in reciprocal space is not exactly along the $\{100\}$ sheets and varies from one Brillouin zone to another in a way which cannot be explained from the present knowledge of the triple-axis spectrometer resolution function.[22] Preliminary study of other perovskites $KMnF_3$ and $SrTiO_3$ near the zone center indicates that this scattering is rather common in perovskite crystals. This poses a rather intriguing question for further investigation of this type of crystals.

ACKNOWLEDGMENT

We would like to express our thanks to Dr. J. D. Axe for many illuminating discussions.

†Work supported by the U. S. Atomic Energy Commission and the National Science Foundation.

*Guest scientist on leave from Service de Physique des Solides associé au CNRS, Faculté des Sciences, 91-Orsay, France (now returned).

[1]G. Shirane, R. Nathans, and V. J. Minkiewicz, Phys. Rev. 157, 396 (1967).

[2]W. Cochran, Advan. Phys. 9, 387 (1960).

[3]J. D. Axe, J. Harada, and G. Shirane, Phys. Rev. B 1, 1227 (1970).

[4]G. Honjo, S. Kodera, and N. Kitamura, J. Phys. Soc. Japan 19, 351 (1964).

[5]R. Comès, M. Lambert, and A. Guinier, Acta Cryst. A26, 244 (1970).

[6]Y. Yamada and G. Shirane, Phys. Rev. 177, 848 (1969).

[7]J. Harada, J. D. Axe, and G. Shirane, Phys. Rev. B 4, 155 (1971).

[8]A. C. Nunes, J. D. Axe, and G. Shirane, Ferroelectrics (to be published).

[9]R. Comès, F. Dénoyer, and M. Lambert, J. Phys. Suppl. (to be published).

[10]S. H. Wemple, Phys. Rev. B 2, 2679 (1970).

[11]M. E. Lines, Phys. Rev. B 2, 690 (1970).

[12]M. Lambert and R. Comès, Solid State Commun. 7, 305 (1969).

[13]T. Riste and K. Otnes, Nucl. Instr. Methods 75, 197 (1969).

[14]Sanders Associates, 95 Canal Street, Nashua, N. H. 03060.

[15]H. H. Barrett, Phys. Letters 26A, 217 (1968).

[16]J. C. Slater, Phys. Rev. 78, 748 (1950).

[17]A. Hüller, Z. Physik 220, 145 (1969).

[18]A. Hüller, Solid State Commun. 7, 589 (1969).

[19]R. Comès, F. Dénoyer, L. Deschamps, and M. Lambert, Phys. Letters 34A, 65 (1971).

[20]K. Gesi, J. D. Axe, G. Shirane, and A. Linz, Phys. Rev. B (to be published).

[21]W. G. Nielsen and J. G. Skinner, Phys. Rev. 47, 1413 (1967).

[22]M. J. Cooper and R. Nathans, Acta Cryst. 23, 357 (1967).

PHYSICAL REVIEW B VOLUME 5, NUMBER 5 1 MARCH 1972

Piezo Soft X-Ray Effect in Nickel

R. H. Willens and D. Brasen
Bell Laboratories, Murray Hill, New Jersey 07974

(Received 4 May 1971)

The modulation of the L_{III} x-ray emission band of nickel due to an alternating mechanical strain is reported. Structure previously not seen in the normal x-ray emission is now resolved, which enables determination of the location of the Fermi energy and other critical points or Van Hove singularities. The bottom of the d band is placed at 5.5 ± 1.0 eV from the Fermi energy. Structure which can be correlated with the spin-exchange energy places its value at 0.68 ± 0.1 eV. The high-energy tails of the L_{II} and L_{III} emission bands contain a satellite which is resolved in the modulation spectrum. The origin of this satellite is attributed to spin-polarization exchange with the $2p$ core states. The experimentally determined value of this exchange is 5.5 ± 0.5 eV.

I. INTRODUCTION

Recently, the modulation of the L_{III} emission spectrum of copper due to an alternating elastic strain was reported.[1] The gross shape of the modulation curve, in the first approximation, had the appearance of the derivative of the emission band. However, superimposed on this curve was additional structure which was associated with positions in the $3d$-$4s$ band of copper which were extra sensitive to strain as regards altering the x-ray emission. These positions were identified with the Fermi energy and Van Hove singularities or critical points.

The L_{III} emission spectrum of nickel (Fig. 1), which corresponds to transitions from the $3d$-$4s$ band to the $2p_{3/2}$ core level, is essentially struc-

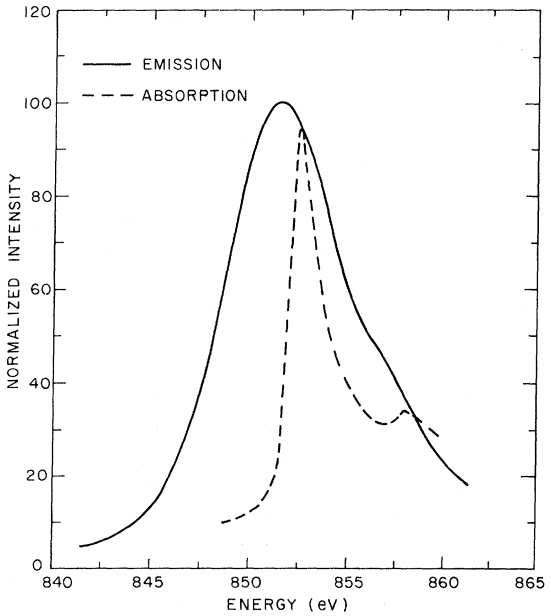

FIG. 1. L_{III} emission band of nickel and the absorption spectrum as measured by Bonnelle (Ref. 3).

tureless with unresolved Van Hove singularities. The peak intensity is located at 851.5 eV.[2] The Fermi energy and lower bound of the band are masked by the high- and low-energy tails. This nickel emission band is quite similar to the copper L_{III} emission except for an additional satellite on the high-energy tail of the nickel emission band. In contrast to copper, the L_{III} absorption edge is quite sharp, and indicates that the Fermi energy is within 1 eV of the peak in the emission band.[3] This leads one to wonder about the possible origin of the large fraction of emission from above the Fermi energy. Liefeld[4] has investigated the Ni L_{III} emission band as a function of excitation voltage. He has determined that the shape of the L_{III} emission band, on the high-energy side, is quite dependent on the energy of the incident electrons, and the excess satellite intensity, on the high-energy tail, decreases with decreasing excitation voltage and is suppressed at voltages just above the L_{III} excitation voltages. It was proposed by Liefeld that L_I and L_{II} ionizations (the $2s_{1/2}$ and $2p_{1/2}$ states) are needed in order to produce the satellite emission. Presumably, these initial ionizations decay by Auger transitions to set up multiple-vacancy states between the L_{III} and M states, which then become the origin of the satellite emissions. Holliday[5] has attempted to duplicate these measurements and finds, contrary to Liefeld's work, that there is no significant reduction of satellite intensity as the voltage is decreased from 4 to 1.45 kV. Holliday attributes the disagreement between his measurements and Liefeld's to the possibility of surface contamination of the nickel sample. Liefeld operates with a sample temperature of 700 °C to eliminate carbon contamination; however, this would not eliminate surface oxidation.[6] Nevertheless, when the L_{III} emission spectra of copper and nickel are compared, two facts are quite evident. First, a large fraction of the emission comes from above the Fermi energy. The origin of this emission, referred to as the high-energy tail, is not fully understood. Second, nickel has an additional satellite. It is doubtful that the origin of this satellite is associated with the occurrence of multiple ionizations, of the type L_{III}-$M_{IV,V}$, produced by Auger transitions, since this process would probably happen to about the same extent in copper and nickel. Arguments will be given later to indicate that the origin of this additional satellite is due to splitting of the $2p_{3/2}$ core level caused by the spin-core exchange with the unpaired conduction electrons.

Earlier[1] it was discovered that by alternating the mechanical strain on a sample of copper and measuring the change in x-ray emission between the strained and unstrained state, it was possible to convert the normal emission spectrum without structural detail into a modulated spectrum with numerous structural details. The reason given for the appearance of this structure in the strain-modulation experiment was the greater sensitivity to strain with regard to altering the x-ray emission, at the Van Hove singularities or critical points. This could be attributed to varying deformation potentials or changes in wave-function mixing at degeneracy points in k space, and consequently transition probabilities, due to the strain altering the lattice symmetry. In addition, it is probable that the mechanism which causes the loss of a good deal of the structure in the x-ray emission band and produces the high-energy tail would have a different derivative of x-ray emission with respect to lattice strain than what could be termed normal band-structure features. Consequently, the Fermi energy, which should be broadened only by the natural lifetime and no intraband Auger broadening, would be indicated by a sharp change in the strain-modulation spectrum.

There is another mechanism for nickel which can result in a change in x-ray emission with the application of a mechanical strain. Nickel is ferromagnetic with the easy direction of magnetization along ⟨111⟩ and the hard direction along ⟨100⟩, and has a crystalline anisotropy constant of about 48 000 erg/cm^3.[7] Also, nickel has an appreciable negative magnetostrictive constant which averages about -35×10^{-6} for polycrystalline material at room temperature.[8] When a mechanical stress is applied to a magnetostrictive material the magnetization of the sample rotates to lower the strain energy of the system. Becker and Döring[9] have derived, for a

material having isotropic magnetostriction and no change of volume upon magnetization, the following equation for the magnetic strain energy:

$$E_\sigma = \tfrac{3}{2}\lambda_S \sigma \sin^2\theta \ ,$$

where λ_S is the magnetostriction constant, σ is the applied stress, and θ is the angle between the direction of magnetization and the stress axis. When the magnetostriction is negative, as in nickel, the total strain energy is a minimum when tension is applied ($\sigma > 0$) for $\theta = \frac{1}{2}\pi$. Therefore tension causes the magnetization to rotate perpendicular to the stress axis, while compression ($\sigma < 0$) causes the magnetization to be parallel to the stress axis. Competing against the rotation of magnetization are the obstacles to domain wall motion and the magnetocrystalline anisotropy. If the stress field is to freely rotate the magnetization, the magnetic strain energy must be greater than the anisotropy energy. The limiting condition for nickel is

$$(E_\sigma)_{\max} = \tfrac{3}{2}\lambda_S \sigma > K \ ,$$

where K is the anisotropy constant. Substituting the appropriate values for nickel, the required stress to overcome anisotropy considerations would be 930 kg/cm^2. This number is only approximate since the nickel samples used in the experimental studies were polycrystalline with varying degrees of texture or preferred orientation. The other obstacle to rotation of the magnetization would be domain wall motion. If the mechanical stress rotates the magnetization and the x-ray emission spectrum is sensitive to rotation of the magnetization, then the degree of cold work of the nickel sample, which would affect domain wall motion, should have a significant effect on strain-modulation results. Later it will be noted that this is what is observed.

The rotation of the magnetization with respect to the crystallographic axes of nickel will vary the spin-orbit splittings of the various nickel subbands. The splittings at the various Van Hove singularities depend on hybridization considerations and magnetic field orientation. The relationship between rotation of the magnetization and spin-orbit splitting has been discussed elsewhere.[10-12] Basically, for the case when the exchange interaction is greater than the spin-orbit interaction, a full spin-orbit splitting of degenerate positions would be expected in a direction parallel to the magnetic induction, and essentially zero splitting at right angles to the magnetic induction. The magnitude of the subband movement as the magnetization rotates would be expected to be of the order of the spin-orbit interaction, 0.12 eV.[10] Shifts of the subbands of this extent are an order of magnitude greater than what could be expected from shifts due to mechanical strain. Additional subband movement is also possible if the alteration in mixing changes the hybridization, which in turn alters the d-d exchange vs s-d exchange.

II. EXPERIMENTAL RESULTS

The technique and apparatus for determining the piezo soft x-ray effect has been previously described in detail.[13] Basically, x rays from the specimen, excited by electron bombardment, are analyzed by a singly bent crystal spectrometer which is step scanned through an emission band. The x rays are observed by the spectrometer normal to the specimen surface to minimize absorption effects. At each step position of the spectrometer the specimen is alternately stressed and unstressed at 10-sec intervals for at least 100 cycles. Between 10^7 and 10^8 counts are accumulated at each step position. The data are recorded on magnetic tape and statistically analyzed, and the difference in intensity between the strained and unstrained states determined. Figure 1 shows the L_{III} emission spectrum of nickel. The data have been normalized to give a peak value of 100. The analyzing crystal was KAP ($2d = 26.8$ Å). Also drawn on the same figure is the absorption spectrum of Ni as measured by Bonnelle.[3] As previously mentioned, there is a large fraction of emission from above what would be considered the Fermi energy as measured by absorption. A small increase in absorption is also noted at about 5.5 eV above the main absorption edge. This is not the L_{II} absorption edge, which is located 17.3 eV higher in energy than the L_{III} edge.

The modulation spectra were obtained on poly-

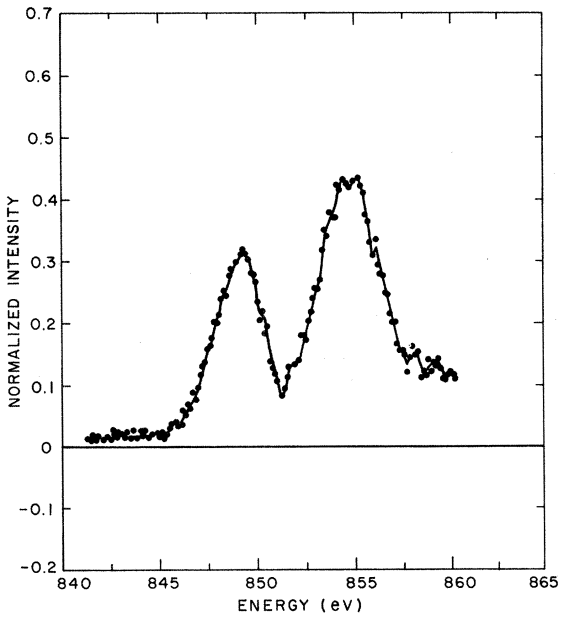

FIG. 2. Change of emission intensity, I_{load}-I_{unload}, as a result of stressing a heavily cold-worked nickel specimen in uniaxial tension to a stress of 850 kg/cm^2.

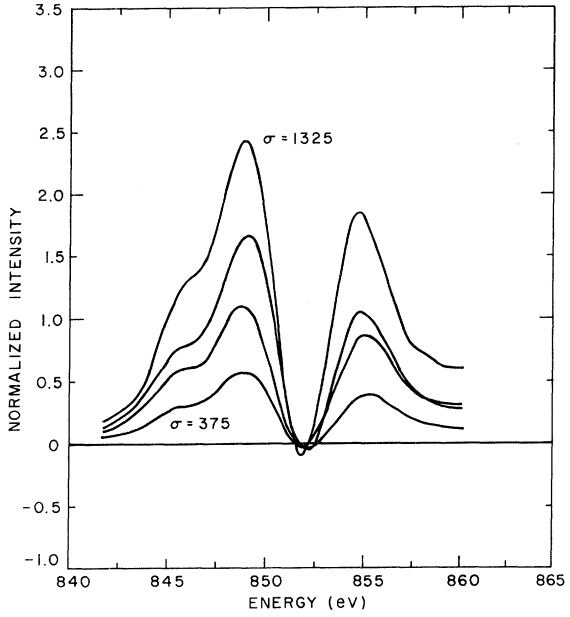

FIG. 3. Modulation spectrum of a nickel specimen at stress levels of 375, 575, 750, and 1325 kg/cm^2, respectively. The specimen was cold worked to about half the extent used to generate Fig. 2.

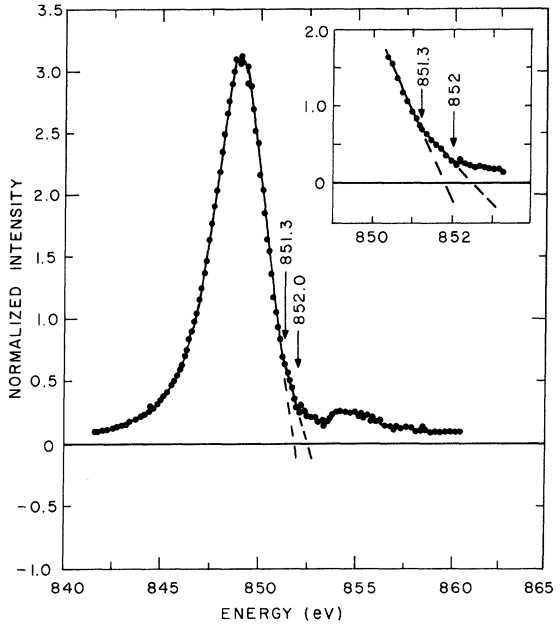

FIG. 5. Modulation spectrum of a nickel specimen loaded in uniaxial tension to a stress of 1150 kg/cm^2.

crystalline samples. The spectra were found to depend upon the individual sample, because of crystallographic orientation effects and the degree of prior cold work given the sample. Figure 2 shows the strain-modulation curve ($I_{\text{load}} - I_{\text{unload}}$) for a nickel sample which was heavily cold worked by rolling. The sample was cyclically loaded in tension to a stress of 850 kg/cm^2. Figure 3 shows a series of modulation curves, at various stress levels, for another sample of nickel which was cold worked to about half the extent used to obtain the modulation curve of Fig. 2. The magnitude of the modulation curve has increased about sevenfold for the same stress level, and the fine structure which is present in Fig. 2 is unresolved. There are two main modulation peaks with an additional piece of structure at about 846 eV on the lower-energy modulation peak. There might also be a small piece of structure on the high-energy modulation peak at about 858 eV. Figure 4 shows how the peak intensity of the modulation curve varies with applied stress. The intensity tends to saturate as the load increases. Higher stress levels could not be applied to this specimen without inducing plastic deformation and a subsequent change in crystallographic texture. The relative and absolute intensities of these modulation peaks vary from sample to sample, presumably from crystallographic texture effects. Of course, the positions of the modulation structure do not vary. Figure 5 shows the modulation curve for another nickel specimen which had the same mechanical cold working as that used to generate the modulation curves illustrated in Fig. 3, but with different crystallographic texture. The sample was cyclically loaded to a stress of 1150 kg/cm^2. For this specimen only one modulation peak is prominent. There are two abrupt changes in slope on the high-energy side of the peak. One occurs at 852.0 eV and the other at 851.32 eV.

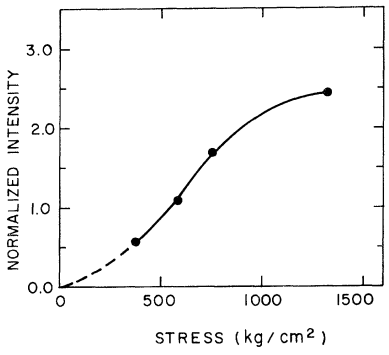

FIG. 4. Variation of the peak intensity of the modulation spectrum with stress.

If a nickel sample is fully annealed, the intensity of the modulation increases to even a greater extent for a given load. Figure 6 shows the modulation curve for an annealed sample cyclically stressed to a level of 575 kg/cm^2 in tension. For this sample the spectrometer was scanned to include the L_{III} and L_{II} ($3d$-$4s$ to $2p_{1/2}$ transition) emission bands. The peak intensity of the modulation curve has in-

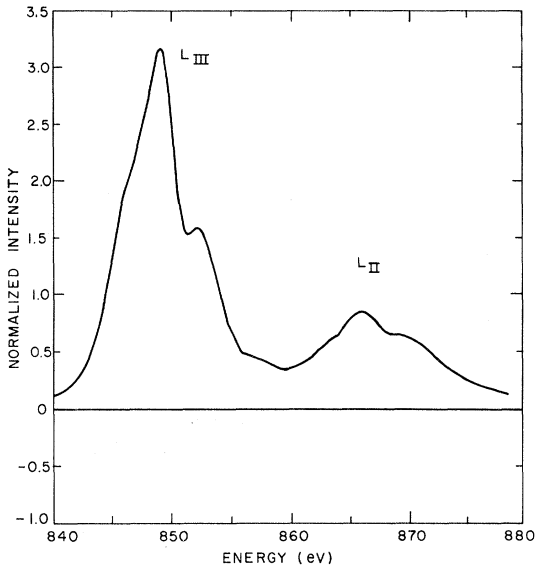

FIG. 6. L_{II} ($2p_{1/2}$) and L_{III} ($2p_{3/2}$) modulation spectra for an annealed nickel specimen loaded in uniaxial tension to a stress of 575 kg/cm^2.

creased to another factor of about 3 from what was observed for the cold-worked sample of Fig. 3. There are only two peaks clearly resolved in the modulation curve for the L_{II} emission band. The corresponding piece of structure on the low-energy side of the L_{III} band is unresolved or absent. The L_{II} modulation curve is broader and reduced in intensity, compared to the L_{III} modulation curve, to approximately the same extent as the ratio of the L_{II} to L_{III} emissions.

III. DISCUSSION

There are several conclusive observations which can be made from Sec. II. First, unlike the results of copper, there are two main modulation peaks. These modulation curves represent the change in x-ray emission between the strained and unstrained condition. Consequently, it is clear that more x-ray emission occurs in this band when the sample is in tension. (Compression was found to reduce the net x-ray emission.) Therefore, the application of the tension must have altered the matrix elements to increase the over-all transition probability between the two states involved in this x-ray transition. Second, as the nickel specimen is annealed the strength of the modulation greatly increases. The magnitude of this increase cannot be reasonably attributed to solely mechanical strain effects. The increase in the modulation appears to be spread throughout the emission band and not mainly associated with critical points or Van Hove singularities as found for mechanical strain modulation. (It has also been found that the addition of copper to nickel, to a concentration which renders it nonmagnetic, has reduced the magnitude of the x-ray modulation to the level that would be expected for mechanical strain.) The origin of this enhanced modulation must be associated with the rotation of the magnetization in the sample due to the strain energy associated with the magnetostrictive effects described earlier. If the volume of the nickel sample, from which the x-ray emission was occurring, had random polycrystalline orientation then there would obviously be no change in the x-ray emission as the magnetization rotates. However, because of the texture which is produced by the cold rolling and annealing, the relative proportions between regions magnetized in different crystallographic directions change with magnetic rotation.

Before attempting to explain the origin of the two main modulation peaks, we believe that the high-energy one is associated with the part of the emission band previously assigned to the "satellite," and the low-energy one is associated with the "normal emission." Since the relative intensities of these two modulation peaks vary from sample to sample, the matrix elements between the conduction–valence band and the two states corresponding to "satellite" and "normal emission" must be different. The separation between these two main modulation peaks is 5.5 ± 0.5 eV. It is interesting to note that the absorption spectrum as measured by Bonnelle[3] and illustrated in Fig. 1 shows structure at this same energy shift above the main absorption edge.

The location of the Fermi energy with respect to the "normal emission" can be estimated from Fig. 2 by extrapolation and separation of the overlapped region between the two modulation peaks, or from Fig. 5 from the position of the abrupt change in slope of the modulation curve. For both cases the abrupt slope change is located at 851.8 ± 0.3 eV. Figure 5 indicates the value most clearly because the intensity of high-energy modulation peak is very small. There are some uncertainties in assigning this value to the Fermi energy. First, the natural breadth of the x-ray transition from the Fermi energy to the $2p_{3/2}$ state and instrumental broadening would tend to lower this value. The natural breadth has been estimated to be about 0.005 eV[14] or 0.5 eV.[15] Next, it is uncertain if the break in the modulation curve should be attributed to the Fermi energy or to some position below the Fermi energy where degeneracy and wave-function mixing are prevalent. However, for nickel these two positions would be approximately equivalent or within the energy which could be resolved. Both the experimental de Haas–van Alphen measurements of Tsui and Stark[16] and the theoretical calculations of Zornberg[10] and of Ruvalds and Falicov[12] reveal that at the Fermi energy along the ΓX

axis near X there are two sets of accidental degeneracies which are eliminated by rotation of the magnetic field. The first high-symmetry point X_2 is located only 0.04 eV below the Fermi energy according to Zornberg. Therefore, it is probable that the Fermi energy lies between 851.4 and 852.0 eV. It is also noted that this is the region where the x-ray absorption, as measured by Bonnelle, is also rapidly increasing.

The modulation spectrum has structure which might also be interpreted as giving a measure of the spin-exchange splitting. The mainly mechanical modulation spectrum of Fig. 2 shows a good deal of structure which could be dissociated into some pairs separated by 0.6 to 0.7 eV, but this is an ambiguous way of deducing the spin-exchange splitting. The magnetic modulation spectrum of Fig. 5 reveals structure which could possibly be a direct measure of the spin-exchange splitting. Referring to Fig. 5, two abrupt changes in slope are noted at 852.0 and 851.32 eV, respectively. Measurements of the slopes of the segments of the modulation curve just below these two energy values reveals that their ratio is 2:1. It is presumed that whatever band-structure feature causes the abrupt change in the x-ray emission at 852.8 eV, this same feature will also be operative at the energy separation of the exchange splitting and will double the rate of the x-ray modulation effect. (If this band-structure feature is spin split above the Fermi energy, doubling would not be observed.) Doubling is observed and the exchange splitting, which is believed to be mainly d-d exchange at this energy level, is

$$\Delta E_d = 0.68 \pm 0.1 \text{ eV} .$$

Although this interpretation may be ambiguous, the experimental value is closely aligned with other estimates. The value of the exchange splitting has been the topic of numerous experimental and theoretical estimates since Slater made his theoretical estimate of 0.55 eV in 1936[17] and later suggested[18] that this should be increased by a factor of $\frac{5}{4}$, to 0.69 eV. A review of the various early estimates of the exchange splitting has been given by Phillips.[19] Recently[10] Zornberg has calculated the band structure of nickel using an interpolation scheme[20] including spin-orbit and exchange interactions. He found that the introduction of a uniform d-d exchange splitting of 0.6 eV results in a consistent interpretation of many of the experimentally measured properties of nickel.

There are two other structural details in addition to the main modulation peak, as can be seen in Figs. 5 and 6: a shoulder on the low-energy side of the main modulation peak at about 846 eV, and a high-energy modulation peak displaced 5.5 eV from the main modulation peak. A clearer indication of the low-energy shoulder can be obtained by subtracting, from the highest stress curve of Fig. 3, the single modulation peak of Fig. 5 scaled to eliminate the main modulation peak. Figure 7 shows the results of the subtraction. The energy scale has been shifted so that the previously determined Fermi energy is set to zero. As can be seen from the figure, this structure is displaced 2.5 ± 1.0 eV from the peak in the modulation curve, or 5.5 ± 1.0 eV below the Fermi energy. Although structure at this energy value has repeatedly appeared in many different types of experimental measurements such as photoemission,[21-24] optical emission,[25,26] and the M_{III} soft x-ray emission,[27] it has been fashionable to attribute this structure to a surface-impurity or surface-plasmon effect unrelated to any band-structure detail. Granted that since the photoemission measurements of Blodgett and Spicer,[21] the magnitude of this peak has gone down with better experimental conditions, and that scattering from impurities or surface-state plasmons undoubtedly do contribute to photoemission in this energy range, this structure has not disappeared entirely. Zornberg's band calculation of Ni indicates that the majority of the d-band density of states lies within 3 eV of the Fermi energy, which would seem to agree with the high-energy photoemission studies of Eastman.[24] However, there is a broadened extension of the d states down another 1.5 eV. The energy-band calculations of Zornberg show a good deal of degeneracy between subbands within 3 eV of the Fermi surface, then a generally open region, and again a clustering around the X_1-X_3 level. The symmetry points for each spin direction are indicated in Fig. 7. The agreement leads one to believe that the low-energy shoulder represents a true band-structure feature.

Now that the 5-eV structure has again revealed itself in another type of measurement, can there be any other possible origin for its presence? One mechanism which can be ruled out is that associated with a surface impurity or surface plasmon with a discrete energy-loss mechanism. Effects from surfaces can generally be ignored for x-ray strain-modulation experiments. The comparatively small fraction of surface to volume participating in x-ray emission, combined with the magnitude of the modulation effect, would place such contamination or surface effects in the noise of the modulation spectrum. If this structure was associated with a discrete loss process, there would be a constant intensity ratio between it and the main modulation peak. Such is not the case. Another possible origin for this structure could be a transition associated with a core-level splitting (which will be discussed later). Although this explanation is possible, the measurements of Cuthill *et al.* of the M_{III} emission spectrum,[27] which indicate structure at the same

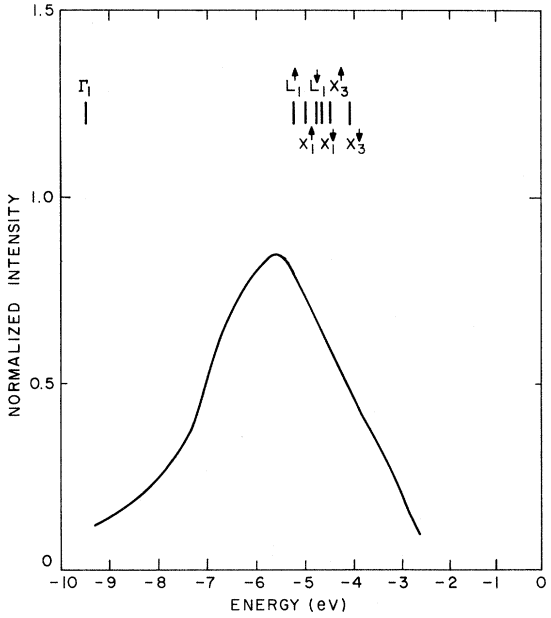

FIG. 7. Low-energy modulation structure obtained by subtracting the scaled modulation curve of Fig. 5 from the highest-stress modulation curve of Fig. 3. The Fermi energy has been set to zero.

energy position, would probably rule this out as a possible mechanism, since the exchange core splittings of the $2p$ and $3p$ levels would be different.

The high-energy modulation peak which occurs 5.5 eV from the main modulation peak is another feature of the spectrum which merits discussion. As shown in Fig. 6, this structure is also present in the L_{II} ($2p_{1/2}$ transition) emission band. As previously mentioned, it is believed that this modulation structure is associated with the satellite on the high-energy emission band. (However for copper, there are no indications of any such structure, above the Fermi energy, in the x-ray strain-modulation experiments.) When the possible origins for this structure are sought, the question arises: Why is this mechanism not applicable to copper? This would seem to rule out any mechanism involving core-state Auger transitions. There are two basic differences between copper and nickel: one, the high density of d-states at the Fermi energy for nickel, and two, the ferromagnetism of nickel.

The fact that this structure occurs at an energy greater than the Fermi energy would seem to indicate that there is a split core level or virtual core level at a lower level than the $2p_{3/2}$ and $2p_{1/2}$ states. The electron spectroscopy for chemical analysis (ESCA) spectrum of the $2p$ core levels, as measured by Baer *et al.*,[28] is shown in Fig. 8. The location of the high-energy x-ray modulation structure, shown in Fig. 6, is at the same relative position as the high-energy structure in the ESCA spectrum. (Structure of this type is absent in the Cu ESCA spectrum.) Baer *et al.* attribute this structure to a discrete energy loss of 5.5 eV associated with a surface plasmon. However, for our case of x-ray emission, there would have to be a discrete energy gain of 5.5 eV. The initial excitation would have to be a $2p_{3/2}$ hole plus plasmon. These would have to mix via a nonlinear process and emit a photon with the sum of the energies. The probability of this process occurring, to be relative magnitude observed in the x-ray modulation experiment, seems very unlikely. Additionally, as previously mentioned, surface states or plasmons should have negligible contributions to the x-ray modulation structure.

The only other alternative for this additional structure, as compared to copper, appears to be a core-level splitting. It is well known[29] that in an atom with a net magnetic moment, there is a spin-polarization exchange with the core levels which splits the spin-up and spin-down states. Unrestricted Hartree-Fock calculations have not been made for metallic nickel, but calculations for Fe indicate that the $2p$ level would have a splitting of 3.2 eV.[30,31] (Recently Fadley *et al.* have observed, by x-ray photoelectron spectroscopy, structure in the $3s$ and $3p$ core states of magnetic Mn and Fe ions which they attributed to the spin-core polarization.[32,33] The order of magnitude for the $3s$ splitting ranged between 4 and 7 eV.) Spin-polarized Hartree-Fock calculations indicate that the $2p$ core levels would be expected to split into doublets. However, a more detailed calculation, including the large spin-orbit interaction, could indicate that the $2p_{3/2}$ would split into a quartet and the $2p_{1/2}$ into a doublet. The magnitude would be related to the expectation of the z component of the spin $|g_j - 1|$. Whether the x-ray modulation curve of the $2p_{3/2}$ level contains another set of unresolved peaks remains an open question for future investigation.

IV. CONCLUSIONS

The modulation of the L_{III} soft x-ray emission of nickel due to an alternating mechanical strain

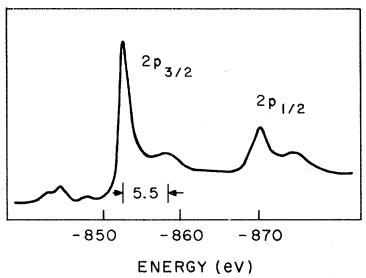

FIG. 8. The core-level ESCA spectrum measured by Baer *et al.* (Ref. 28).

has produced structure which can be correlated with the following details of the electronic structure: (i) The heretofore unresolved Fermi energy was located at 851.8 ± 0.4 eV. (ii) Structure attributed to the spin-exchange splitting, places its measured value at 0.68 ± 0.1 eV. (iii) The modulation spectrum from heavily cold-worked nickel indicates energy values for the high symmetry or multiple-degeneracy positions. (iv) There is band-structure detail 5.5 ± 1.0 eV below the Fermi energy which is probably the bottom of the d band. (v) The high-energy tail of the L_{II} and L_{III} emission bands, which probably includes effects of other broadening processes such as multiple ionizations resulting from Auger transitions, has a satellite located 5.5 ± 0.5 eV from the main emission peak and is probably a measure of the spin-polarization exchange with the $2p$ core states.

ACKNOWLEDGMENTS

The authors would like to express their appreciation to C. Herring, P. W. Anderson, J. C. Phillips, and L. F. Mattheiss for the helpful discussions concerning the interpretation of the data. Also, thanks are given to J. H. Wernick for advice and encouragement and to H. Schreiber for experimental assistance.

[1]R. H. Willens, H. Schreiber, and D. Brasen, Phys. Rev. Letters 23, 413 (1969).
[2]J. A. Bearden, Rev. Mod. Phys. 39, 78 (1967).
[3]C. Bonnelle, in *Soft X-Ray Band Spectra*, edited by D. J. Fabian (Academic, New York, 1968), p. 163.
[4]R. J. Liefeld, in *Soft X-Ray Band Spectra*, edited by D. J. Fabian (Academic, New York, 1968), p. 133.
[5]J. E. Holliday, in *Advances in X-Ray Analysis*, edited by B. L. Henke, J. E. Newkirk, and G. R. Mallett (Plenum, New York, 1970), Vol. 13, p. 136.
[6]A. U. MacRae, Surface Sci. 1, 319 (1964).
[7]H. J. Williams and R. M. Bozorth, Phys. Rev. 55, 673 (1939).
[8]R. M. Bozorth, *Ferromagnetism* (Van Nostrand, New York, 1951), p. 659.
[9]R. Becker and W. Döring, *Ferromagnetismus* (Springer, Berlin, 1939).
[10]E. I. Zornberg, Phys. Rev. B 1, 244 (1970).
[11]E. Abate and M. Asdente, Phys. Rev. 140, A1303 (1965); L. Hodges, D. R. Stone, and A. V. Gold, Phys. Rev. Letters 19, 655 (1968); A. V. Gold, J. Appl. Phys. 39, 768 (1968).
[12]J. Ruvalds and L. M. Falicov, Phys. Rev. 172, 508 (1968).
[13]R. H. Willens, in *Electronic Density of States*, edited by L. H. Bennett, Natl. Bur. Std. (U.S.) Spec. Publ. 323 (U.S. GPO, Washington, D.C., 1971).
[14]James H. Scofield, Phys. Rev. 179, 9 (1969).
[15]L. G. Parratt, Rev. Mod. Phys. 31, 616 (1959).
[16]D. C. Tusi and R. W. Stark, Phys. Rev. Letters 17, 871 (1966); D. C. Tusi, Phys. Rev. 164, 669 (1967).
[17]J. C. Slater, Phys. Rev. 49, 537 (1936).
[18]J. C. Slater, J. Appl. Phys. 39, 761 (1968).
[19]J. C. Phillips, J. Appl. Phys. 39, 755 (1968).
[20]L. Hodges, H. Ehrenreich, and N. D. Lang, Phys. Rev. 152, 505 (1966); F. M. Mueller, *ibid.* 153, 569 (1967).
[21]A. J. Blodgett, Jr. and W. E. Spicer, Phys. Rev. Letters 15, 29 (1965).
[22]T. A. Callicott and A. U. MacRae, Phys. Rev. 178, 966 (1969).
[23]D. T. Pierce and W. E. Spicer, Phys. Rev. Letters 25, 581 (1970).
[24]D. E. Eastman, J. Appl. Phys. 40, 1387 (1969).
[25]H. Ehrenreich, H. R. Philipp, and D. J. Olechna, Phys. Rev. 131, 2469 (1963).
[26]M. Shiga and G. P. Pells, J. Phys. C 2, 1835 (1969).
[27]J. R. Cuthill, A. J. McAlister, M. L. Williams, and R. E. Watson, Phys. Rev. 164, 1006 (1967).
[28]Y. Baer, P. F. Hedén, J. Hedman, M. Klasson, C. Nordling, and K. Siegbahn, Physica Scripta 1, 55 (1970).
[29]J. C. Slater, *Quantum Theory of Atomic Structure* (McGraw-Hill, New York, 1960), Vol. 2.
[30]P. S. Bagus and B. Liu, Phys. Rev. 148, 79 (1966).
[31]J. C. Slater, Phys. Rev. 165, 658 (1968).
[32]C. S. Fadley, D. A. Shirley, A. J. Freeman, P. S. Bagus, and J. V. Mallow, Phys. Rev. Letters 23, 1397 (1969).
[33]C. S. Fadley and D. A. Shirley, Phys. Rev. B 2, 1109 (1970).